以立體微流道製作雙重乳化三相微囊胞

Controlled W/O/W Double Emulsification in 3-D PDMS Micro-Channels

本研究利用疏水性高分子材料製作立體微流道，搭配介面活性劑以限制油相流體在流道表面的濕潤範圍，並維持各相間介面的穩定，成功產生水油水三相雙重乳化微囊胞。微囊胞的外徑大小、油相球殼厚度、與水相核心大小可以透過水油水三相流速控制，另外微囊胞的產生機制與頻率則可藉由流道形狀加以限制。

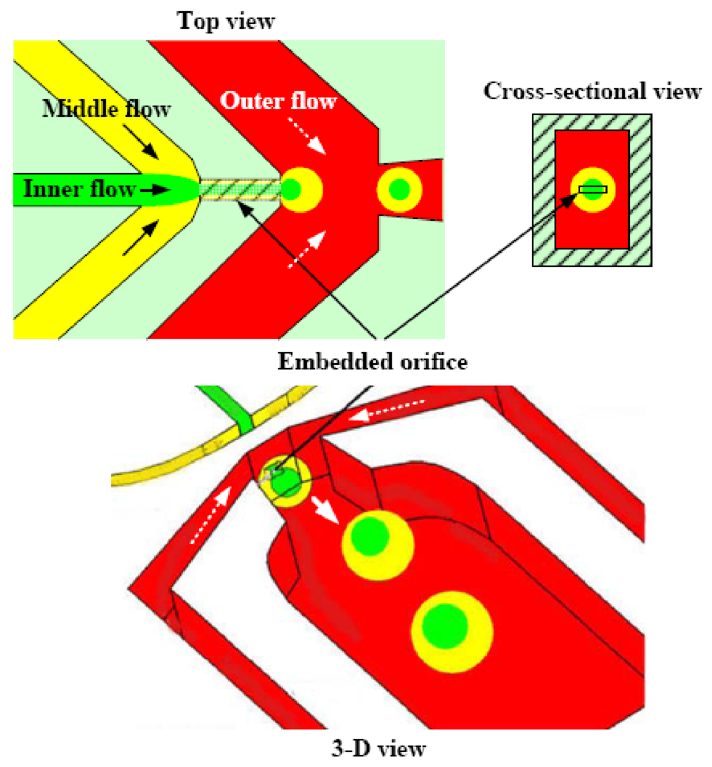

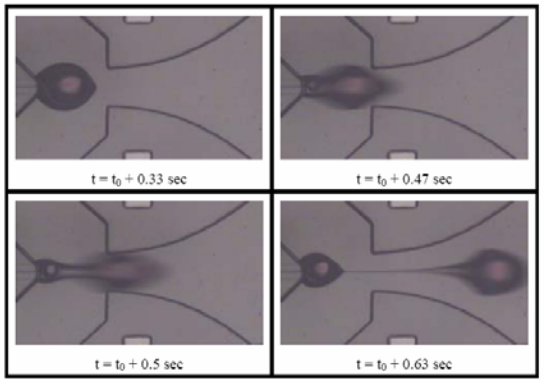

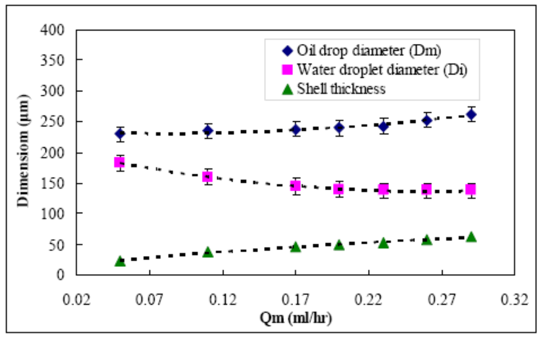

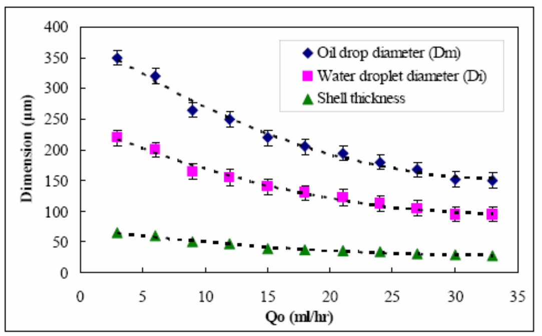

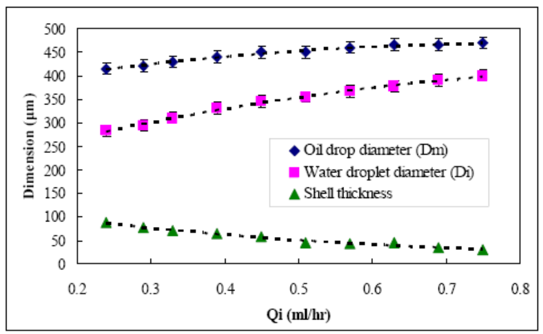

IOP PUBLISHING JOURNAL OF MICROMECHANICS AND MICROENGINEERING

J. Micromech. Microeng. **18** (2008) 065018 (8pp) doi:10.1088/0960-1317/18/6/065018

Controlled double emulsification utilizing 3D PDMS microchannels

Fu-Che Chang and Yu-Chuan Su

Department of Engineering and System Science, National Tsing Hua University, Hsinchu, Taiwan

E-mail: ycsu@ess.nthu.edu.tw

Received 30 December 2007, in final form 14 April 2008
Published 9 May 2008
Online at stacks.iop.org/JMM/18/065018

Abstract

This paper presents a PDMS emulsification device that is capable of generating water-in-oil-in-water double emulsions in a controlled manner. Specially designed 3D microchannels are utilized to steer the independently driven water- and oil-phase flows (especially to restrict the attachment of the middle oil-phase flow on the channel surfaces), and to break the continuous flows into monodisperse double emulsions. In addition to channel geometries and fluid flow rates, surfactants and osmotic agents are employed to facilitate the breakup process and stabilize the resulting emulsion structures. In the prototype demonstration, two-level SU-8 molds were fabricated to duplicate PDMS microstructures, which were surface treated and bonded irreversibly to form 3D microchannels. Throughout the emulsification trials, dripping was intentionally induced to generate monodisperse double emulsions with single or multiple aqueous droplets inside each oil drop. It is found that the overall and core sizes of the resulting double emulsions could be adjusted independently, mainly by varying the outer and inner fluid flow rates, respectively. As such, the presented double emulsification device could potentially realize the controllability on emulsion structure and size distribution, which is desired for a variety of biological and pharmaceutical applications.

(Some figures in this article are in colour only in the electronic version)

Introduction

Mixing immiscible fluids together results in an emulsion, which might be defined as a heterogeneous system consisting of at least one fluid (in the form of tiny droplets) dispersed within another fluid [1]. An emulsion does not form spontaneously. It is produced by an emulsification process, through which interfaces between fluids are created and stabilized by some emulsifying agents [2]. Monodisperse emulsions are highly desirable for a variety of applications, including agriculture, petroleum industry and pharmaceutical products [1–4]. Previously, various microfluidic emulsification schemes such as T-junctions [5–7] and flow-focusing devices [8–13] had been demonstrated to be capable of generating emulsions in a consistent and controllable manner. Regardless of the mechanism, the formation of emulsions usually depends on the wetting properties of the employed fluids on the channel materials. For example, water-in-oil emulsions usually form in channels with hydrophobic surfaces, while stable formation of oil-in-water emulsions generally occurs in channels made of hydrophilic materials [14–16].

Double emulsions are structured fluids that consist of emulsion drops with smaller droplets inside. With the employment of a middle fluid, the inner fluid is completely separated from the outer continuous-phase fluid. Compared to simple emulsions, double emulsions are inherently more difficult to form and stabilize, because more phases and interfaces are involved in the emulsification process. Conventionally, two-step emulsification processes, in which the inner droplets are emulsified in the middle fluid first and the mixture is then emulsified in the outer continuous-phase fluid, are employed for the massive production of double emulsions [2, 17]. However, the results are usually ill-controlled in both size and structure, owing to the polydispersity resulting from the processes. Because of the strong application potential, such as the encapsulation of drugs [18, 19] and living cells [20–22], considerable attention has been attracted to the development of controllable and reliable fabrication schemes for double emulsions. Recently, researchers have demonstrated double emulsification in various microfluidic devices utilizing two-step droplet breakup [16, 23] and three-dimensional flow focusing [24–27]. To achieve double emulsification, the two-step breakup approaches often employ special surface treatment to definite the required hydrophobic and hydrophilic patterns, while the flow-focusing schemes usually utilize manual assembly of nozzles (or capillary tubes) or complicated fabrication processes to construct the desired 3D structures. Both the surface treatment and manual (or serial) assembly processes could result in high manufacturing cost and limited reliability, and therefore hinder the practical application of these demonstrated devices. Furthermore, the difficulty in integrating the surface treatment or manual assembly process with the fabrication of common microfluidic systems has restricted the application of these demonstrated approaches.

To address the need for simplicity and flexibility, this paper presents a PDMS emulsification device that employs specially designed, 3D microchannels to generate water-in-oil-in-water double emulsions in a controlled manner. Two-level PDMS layers, which are duplicated utilizing a standard casting process, are bonded irreversibly to form the desired 3D microstructures. Three achievements have been accomplished: (1) the design of 3D PDMS microchannels that can steer and break independently driven water- and oil-phase flows into monodisperse double emulsions; (2) the development of a fabrication process that can massively duplicate the 3D PDMS microstructures for double emulsification and (3) the implementation of a PDMS emulsification device that can generate water-in-oil-in-water double emulsions with desired emulsion structure and size distribution. As such, the proposed PDMS microfluidic devices could readily serve as versatile and low-cost emulsification tools, which are desired for various biological and pharmaceutical applications.

Operating principle

A schematic illustration of the proposed 3D microchannels for water-in-oil-in-water double emulsification is shown in figure 1, in which the detailed geometries of two adjacent focusing junctions with one embedded orifice connecting in between are illustrated. The employed inner, middle and outer fluids are driven by three independently controlled syringe pumps operating at varying flow rates. Before entering the embedded orifice, the inner water-phase flow is intersected and focused by the middle oil-phase flow at the upstream junction. While flowing inside the embedded orifice, the inner water-phase flow is either shaped into a thread or broken into a series of droplets by the surrounding oil-phase flow, depending mainly on the flow rates and viscosities of the fluids involved [14]. As already demonstrated by prior 3D flow-focusing works [28, 29], the embedded orifice (located in the sidewall separating the two adjacent focusing junctions) is utilized to restrict the water-in-oil coaxial flow away from the surfaces of the downstream channel. Once coming out of the embedded orifice, the water-in-oil coaxial flow is intersected and focused by the outer water-phase flow, without touching the downstream channel surfaces. Ideally, with the assistance of viscous and/or inertial forces that act against interfacial tension, the water-in-oil coaxial flow could be broken into drops with water-in-oil-in-water structure [26]. However, if the middle oil-phase flow is not appropriately focused away from the downstream channel surfaces, it is expected that the attachment of the oil-phase flow on the hydrophobic PDMS surfaces would distort the flow pattern and eventually result in the failure of double emulsification. For an on-chip focusing and emulsification configuration, the use of an embedded orifice is anticipated to reduce the undesired surface distraction significantly.

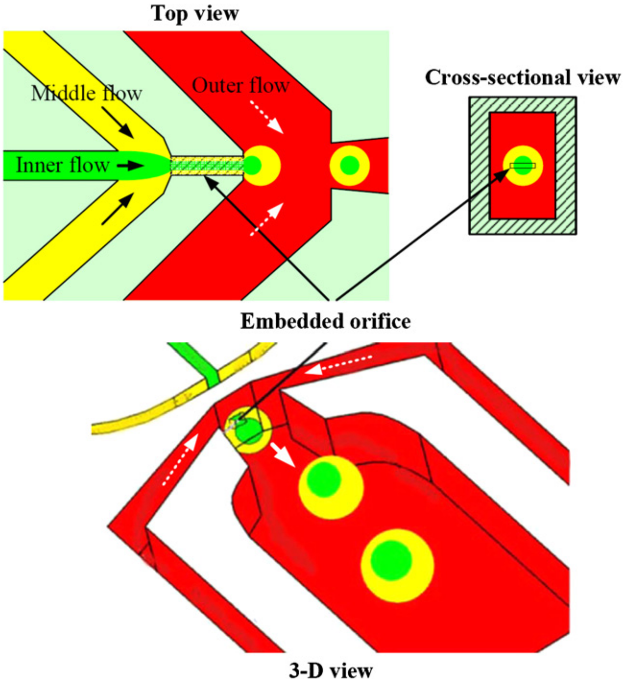

Figure 1. Schematic illustration of the proposed 3D microchannels for double emulsification.

Emulsions are not in equilibrium, but their stability could be greatly improved by the employment of surfactants. Because of the involvement of one extra interface, double emulsions are inherently less stable than simple emulsions are. To stabilize the two interfaces between the middle oil-phase fluid and the inner and outer water-phase fluids, one surfactant suitable for water-in-oil emulsions and another one suitable for oil-in-water emulsions are dispersed in the middle oil-phase and the outer water-phase fluids, respectively. Meanwhile, the employment of surfactants could also adjust the wettability of the oil-phase and water-phase fluids on PDMS surfaces. For hydrophobic PDMS channels, it is most likely that the middle oil-phase fluid, whose interfacial tension with PDMS is much lower than that of the outer water-phase fluid, would attach itself to the channel surfaces. The utilization of the embedded orifice could potentially prevent the attachment, but it is quite possible that some unexpected disturbance during the operation (especially the starting period) might still lead to the undesired attachment and halt the emulsification process immediately. With the addition of surfactant molecules

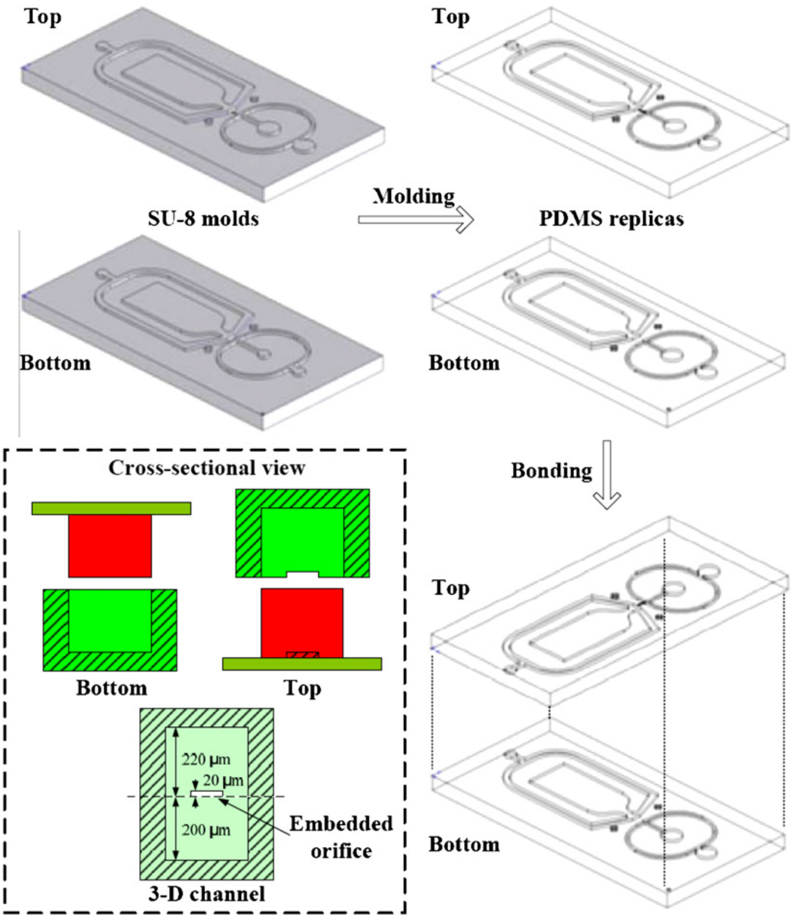

Figure 2. Fabrication process of the proposed 3D microfluidic channels.

into the outer water-phase fluid, its wettability on PDMS surfaces could be improved and the undesired attachment could possibly be eliminated, simply by accelerating the outer water-phase flow to detach the middle oil-phase flow from the PDMS sidewalls.

The breakup of a continuous flow into dispersed droplets usually resulted from the interaction of viscous stresses associated with the imposed flow field, and capillary stresses due to the surface tension between two fluids. Generally, there are two types of droplet-formation mechanisms: dripping and jetting [30, 31]. Dripping produces droplets, which are usually highly monodisperse, close to the exit of the embedded orifice. In contrast, jetting produces a long jet that extends into the downstream channel, where it breaks into polydisperse droplets. The behavior is usually determined by the capillary number, which reflects the balance between the drag of the outer fluid pulling the droplet downstream and the interfacial tension resisting the flow as pinch-off occurs. Aiming to produce monodisperse droplets, which are most likely resulted from dripping, the downstream channel close to the exit of the embedded orifice is narrowed down to roughly three times wider than the orifice is. The abrupt reduction in channel width could potentially accelerate the fluid flow rates and lateral perturbation around the exit of the orifice, and therefore facilitate the preferable dripping breakup. Meanwhile, a highly viscous oil-phase fluid (oleic acid), which has a viscosity of roughly 30 times higher than that of the inner and outer water-phase fluids, is employed as the middle oil-phase fluid to encapsulate aqueous droplets. With the high viscosity, dripping breakup could be induced over a wide range of fluid flow rates [32]. As such, double emulsions with uniform size distribution could be produced at raised breakup frequencies and over a wide range of fluid flow rates. Once passing through the narrow gap, droplets are decelerated in the downstream diverging channel, where they could be further processed or temporally stored.

Fabrication processes

Two-level photolithography, PDMS molding and irreversible PDMS bonding processes (similar to several previous works [33–35]) were employed to fabricate the proposed 3D microchannels for prototype demonstration, as illustrated in figure 2. First of all, a layer of 200 μm thick negative photoresist (SU-8, MicroChem) was spin-coated and patterned on top of a clean silicon wafer to fabricate the mold used for duplicating the bottom layer of PDMS microchannels. Meanwhile, the mold used for duplicating the top PDMS layer, which has microchannels of two different depths on it, was fabricated by coating and patterning a 20 μm thick SU-8 layer first, followed by a second SU-8 layer of 200 μm in thickness. After the SU-8 molds were fully cured, they were placed in a desiccator under vacuum for 2 h with a vial containing a few drops of 1H,1H,2H,2H-perfluorooctyl-trichlorosilane (Fluka) to silanize the surfaces. The purpose of this silanization step is to facilitate the removal of polymeric replicas (from the molds) after the following casting process. A mixture of 10:1 PDMS pre-polymer and curing agent (Sylgard 184, Dow-Corning) was stirred thoroughly and then degassed under vacuum to remove trapped air bubbles. The pre-polymer and curing agent mixture was then poured onto the molds, degassed and cured for 2 h at 85 °C. After thoroughly cured, the PDMS replicas were peeled off from the molds.

Once peeled off from the mold, the top PDMS layer was punched through with a sharp metal-tube array to fabricate the connecting holes for three inlets and one outlet, and ultrasonically cleaned in an ethanol bath to remove residual debris from its surface. The surfaces of the two PDMS layers were then treated with a hand-held corona treater (BD-20AC, Electro-Technic Products), which ionizes surrounding air and creates localized plasma to activate the surfaces for irreversible bonding. The intensity of the corona was set at a relatively low level in order to produce a stable but soft corona with minimal crackling and sparking [36]. The wire electrode was positioned roughly 3 mm above the treated surface and scanned back and forth for 30 s to 1 min, depending on the size of the surface. The corona-treated surfaces were then pressed together and left undisturbed for at least 1 h at 85 °C for the bonding to take effect. At the end, PTFE tubes were inserted into the punched holes to build the necessary interconnection for sample injection and discharge.

Experimental details

Water-in-oil-in-water double emulsions were prepared using oleic acid (Aldrich, with a viscosity of 27.64 mPa s) with 5 wt% of Span 80 (Aldrich) as the middle oil-phase fluid. Meanwhile, deionized water was used as the inner and outer water-phase fluid, with 10 wt% of glycerol (Aldrich) and 5 wt% of Tween 20 (Aldrich) dissolved within, respectively. The three fluids were injected into a fabricated PDMS microfluidic device (as the one shown in figure 3) with the sequence illustrated in figure 4, while the fluid flow rates were controlled independently by three syringe pumps (Model 200, KDS). The outer water-phase fluid was injected into the device first, followed by the injection of the middle oil-phase fluid. Meanwhile, the flow rates of the two fluids were increased slowly, until stable oil-in-water emulsification was reached. Finally, the inner water-phase fluid was injected into the device, with a slowly increasing flow rate. As such, stable emulsification could eventually be reached and the flow rates were adjusted afterward to characterize their effects on emulsification behavior. The formation of double emulsions was observed under an optical microscope and images were recorded using a computer-controlled CCD camera.

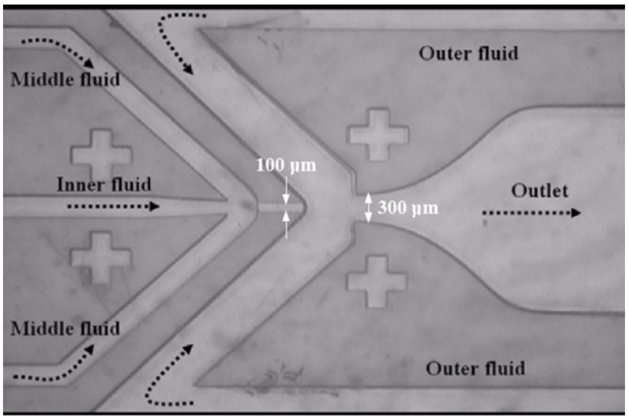

Figure 3. Photograph of the fabricated 3D emulsification device.

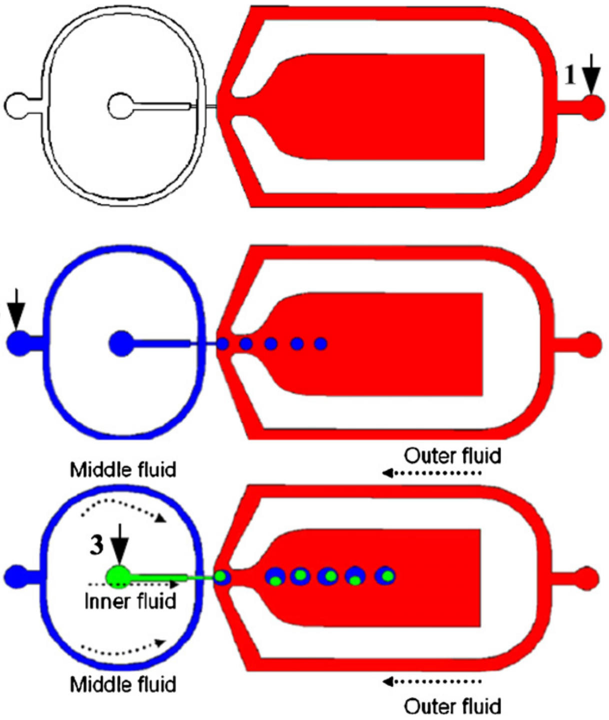

Figure 4. Fluid injection sequence: (1) outer water-phase fluid, (2) middle oil-phase fluid and (3) inner water-phase fluid.

Results and discussion

Prior to the emulsification trials, the wettability changes caused by the addition of surfactants were first characterized, and the results are illustrated in figure 5. It was measured that the contact angle of a water drop with 5 wt% Tween 20 on a PDMS surface is 81.5°, which is 11.9° less than that of a pure water drop. Meanwhile, the contact angle of an oleic acid drop with 5 wt% Span 80 on a PDMS surface was measured to be 49.5°, which is 3.1° more than that of a pure oleic acid drop. In the following emulsification trials, a water-in-oil coaxial flow was formed inside the embedded orifice, and focused away from the downstream PDMS sidewalls as shown in figure 6. At an inner-to-middle flow-rate ratio ($Q_\mathrm{i}/Q_\mathrm{m}$) higher than a

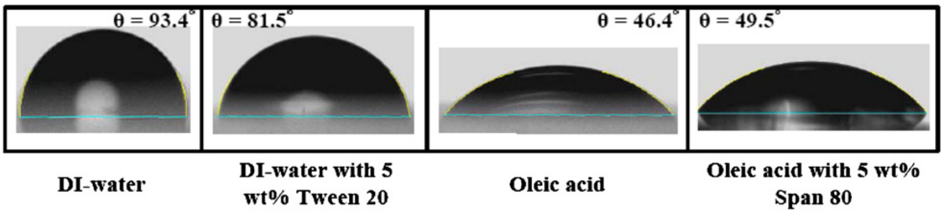

Figure 5. Comparison of the wettability of DI water and oleic acid on PDMS surfaces before and after surfactants are added.

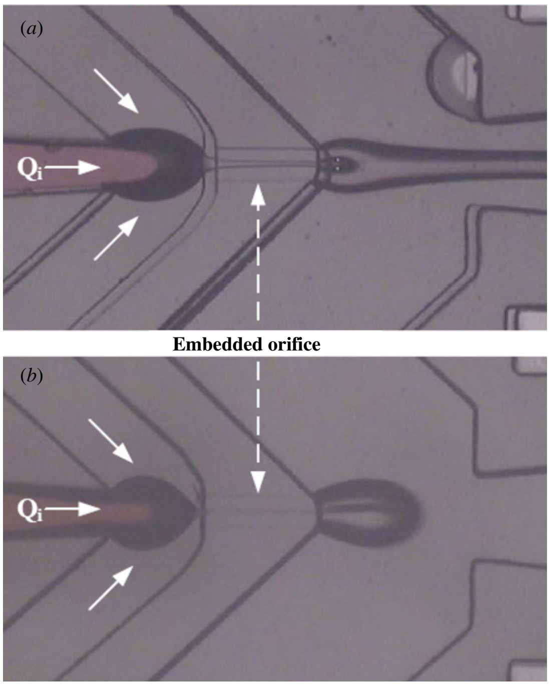

Figure 6. Geometries of inner water-phase flows inside embedded orifices: (*a*) a thread when the Q_i/Q_m ratio is high and (*b*) a series of dispersed droplets when the Q_i/Q_m ratio is low.

certain threshold, the inner water-phase flow was shaped into a thread while flowing through the embedded orifice. In cases that Q_i/Q_m was lower than the threshold, the inner water-phase flow was broken into a series of droplets by its surrounding oil-phase flow. The length-to-width ratio of the embedded orifice is a key geometrical factor that affects the Q_i/Q_m threshold, and therefore the size and number of the aqueous droplets resulted inside each oil drop. It was verified that at the same fluid flow rates, an emulsification device with a long embedded orifice would be more likely to result in double emulsions with multiple aqueous droplets inside each oil drop.

Figure 7 shows a typical double emulsification sequence captured under a microscope. In this case the inner (Q_i), middle (Q_m), and outer (Q_o) fluid flow rates are 0.05, 0.15 and 4 ml h^{-1}, respectively, and the emulsification period is found to be 0.7 s. In a cycle beginning at t_0, the front of the water-in-oil coaxial flow was held around the exit of the embedded orifice until $t_0 + 0.47$ s, when the front moved into a convergent channel and was accelerated downstream. At this moment, it was observed that the less viscous inner water-phase flow had already been broken, while the more viscous middle oil-phase flow was just slightly stretched. The velocity gradient along the flow direction eventually stretched the middle oil-phase flow into a long thread with an aqueous droplet in its front end, and finally broke it into an oil drop with just one water droplet inside. The breakup frequency can be adjusted by varying the fluid flow rates. For example, when Q_i, Q_m and Q_o are 1.5, 1 and 20 ml h^{-1}, respectively, the breakup frequency is raised to around 85 Hz. As shown in figure 8, the middle oil-phase flow was a long jet before the inner water-phase flow was introduced, while the breakup switched to dripping mode once the inner water-phase flow was injected.

It was also observed that by varying the flow rates of the three involved fluids (Q_i, Q_m and Q_o), the overall (D_m) and core (D_i) diameters of the resulting double emulsions could be adjusted. In general, the overall diameter (D_m) of the resulting oil drops is mainly determined by the outer fluid flow rate (Q_o). The overall diameter (D_m) decreases in case that a higher outer fluid flow rate is employed, while the core diameter (D_i) and breakup period decrease as well. Figure 9 illustrates the measured relationship between the outer fluid flow rate (Q_o) and the resulting emulsion dimensions. The flow rates of the inner and middle fluids were set at 0.05 and 0.15 ml h^{-1}, respectively, while the outer fluid flow rate (Q_o) was varied from 3 to 33 ml h^{-1}, which resulted in water-in-oil-in-water emulsions of 350–150 μm in diameter. Further increase in the outer fluid flow rate (Q_o) would eventually switch the breakup to jetting mode, which usually leads to polydisperse results and is beyond the scope of this work. Meanwhile, the size deviations of the resulting emulsions are found to be less than 7.5% of the corresponding average values, as listed in table 1. Figure 10 illustrates the measured relationship between the middle fluid flow rate (Q_m) and the resulting emulsion dimensions, when the flow rates of the inner (Q_i) and outer (Q_o) fluids were set at 0.05 and 10 ml h^{-1}, respectively. It was found that the increase in the middle fluid flow rate (Q_m) resulted in the increase in the overall diameter (D_m), even though the breakup period decreased. The overall diameter (D_m) rose from 230 to 260 μm, while the sum of the inner (Q_i) and middle (Q_m) flow rates rose 3.5 times from 0.1 to 0.35 ml h^{-1}. Meanwhile, the core diameter (D_i) decreased because of the decrease in the breakup period. Further increase in the middle fluid flow rate (Q_o) would eventually result in an oil-in-water coaxial flow with aqueous droplets inside the oil phase. On the other hand, it was found that the rise of the inner fluid flow rate (Q_i) resulted in the increase in the overall diameter (D_m). Figure 11 illustrates the measured relationship between the inner fluid flow rate (Q_i) and the

Table 1. Measured emulsion dimensions and deviations at various outer fluid flow rates.

Q_o (ml h^{-1})	3	6	9	12	15	18	21	24	27
Average D_m (μm)	351	322	264	249	218	205	194	182	168
Std deviation (%)	4.20	4.75	4.63	5.73	4.39	5.68	5.83	7.12	6.28
Average D_i (μm)	220	202	163	157	141	129	123	114	105
Std deviation (%)	4.35	5.21	4.93	5.51	5.81	6.03	7.29	6.61	6.47

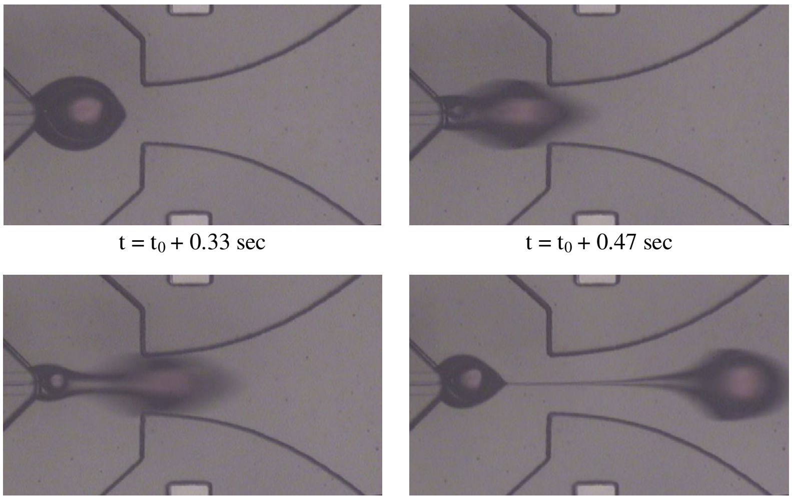
t = t$_0$ + 0.33 sec

t = t$_0$ + 0.47 sec

t = t$_0$ + 0.5 sec

t = t$_0$ + 0.63 sec

Figure 7. A captured double emulsification sequence.

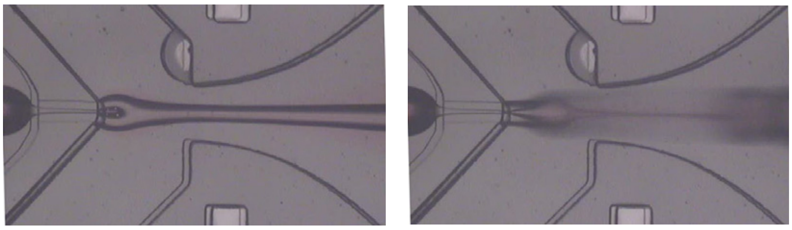
(*a*)

(*b*)

Figure 8. Captured high-frequency emulsification (*a*) before and (*b*) after the inner water-phase fluid was injected.

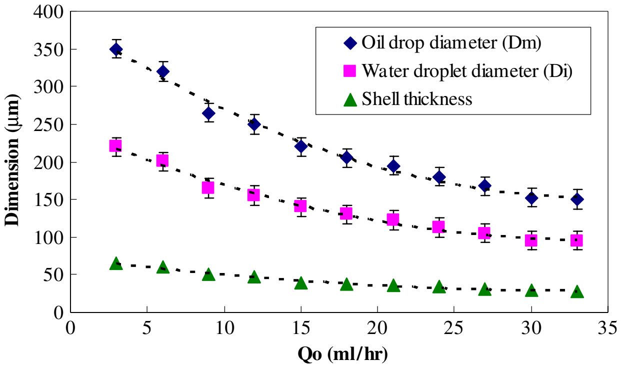

Figure 9. Relationship between emulsion dimensions and outer fluid flow rates.

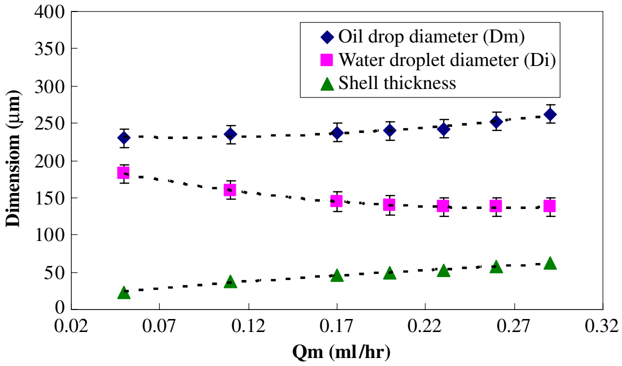

Figure 10. Relationship between emulsion dimensions and middle fluid flow rates.

resulting emulsion dimensions, when the flow rates of the middle (Q_m) and outer (Q_o) fluids were set at 0.5 and 3 ml h^{-1}, respectively. Even though the break-up period decreased when the inner fluid flow rate (Q_i) rose from 0.24 to 0.75 ml h^{-1}, the overall diameter (D_m) rose from 415 to 470 μm. Further increase in the inner fluid flow rate (Q_i) would eventually

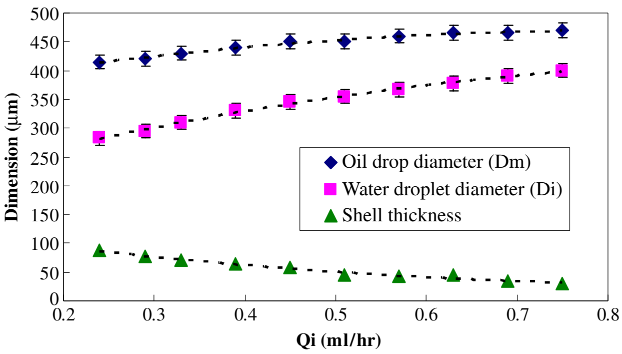

Figure 11. Relationship between emulsion dimensions and inner fluid flow rates.

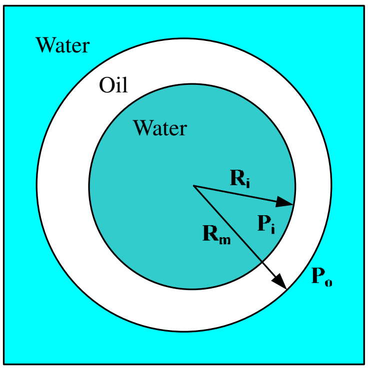

$$P_i - P_o = 2\gamma\left(\frac{1}{R_i} + \frac{1}{R_m}\right)$$

Figure 12. Laplace pressure between two water-phase fluids separated by an oil-phase shell.

result in the failure of double emulsification, while a high-speed water jet bursts the middle oil-phase flow. Therefore, it is recommended that the inner fluid flow rate should be adjusted from low to high at the last, after stable oil-in-water emulsification with the desired drop diameter (D_m) is roughly achieved inside the microchannels. The inner (Q_m) and middle (Q_i) fluid flow rates are then reduced and raised, respectively, to adjust the water-to-oil volume ratio of the produced double emulsions.

In addition to the properties of the employed surfactants, the stability of the resulting double emulsion is also dependent on the pressure gradient across the oil-phase shell. As shown in figure 12, the pressure inside the inner water phase is by definition higher than that in the outer water phase [37]. This pressure gradient might result in water loss across the oil-phase shell, and eventually the structural degradation from double to single emulsion. In order to balance the pressure gradient and to prevent the potential structural degradation, ingredients (or osmotic agents) with proper chemical properties needed to be included in the inner water-phase fluid. The resulting chemical potential (or osmotic pressure) gradient would act against the Laplace pressure and stop the potential water loss. With an oleic acid drop diameter (D_m) of roughly 100 μm, the Laplace pressure ($P_i - P_o$) across the oil-phase shell is estimated to be no less than 1.2 kN m^{-1}, which would be higher in cases that smaller aqueous droplets are encapsulated inside the oleic acid drop. In our emulsification trails, glycerol was dissolved in the inner water-phase fluid to raise both the viscosity of the inner flow and the osmotic pressure inside the encapsulated water droplets. It is found that a minimal 30 wt% glycerol is needed in order to stabilize the double emulsion for an extended period of time. Otherwise, the structure collapses when the inner and outer water-to-oil interfaces come into contact. Meanwhile, the viscosity of the inner water-phase flow is found to be proportional to the glycerol concentration. With a higher inner-fluid viscosity, dripping breakup could be induced over a wider range of fluid flow rates. The resulting drop size is found to be relatively small, compared to that of the case while pure DI water and the same fluid flow rates are employed.

Conclusion

This work demonstrates a PDMS emulsification device that is capable of generating water-in-oil-in-water double emulsions in a controlled manner. Specially designed, 3D microchannels are employed to steer the three-phase flow, which is driven by three independently controlled syringe pumps, and break the continuous flows into monodisperse double emulsions. In addition, surfactants and osmotic agents are employed to facilitate the breakup process and stabilize the resulting emulsion structures. In the prototype demonstration, two-level SU-8 molds were fabricated to duplicate PDMS microstructures, which were surface treated and bonded irreversibly to form 3D microchannels. Dripping was intentionally induced by channel geometries and fluid flow rates to generate monodisperse double emulsions with oleic acid as the middle oil-phase fluid. It is found that the overall and core sizes of the resulting double emulsions could be adjusted independently, mainly by varying the outer and inner water flow rates, respectively. Three accomplishments have been achieved: (1) the design of 3D PDMS microchannels that can steer and break independently driven water and oil-phase flows into monodisperse double emulsions; (2) the development of a fabrication process that can massively duplicate the 3D PDMS microstructures for double emulsification; and (3) the implementation of a PDMS emulsification device that can generate water-in-oil-in-water double emulsions with desired emulsion structure and size distribution. As such, the demonstrated double emulsification device could potentially realize the controllability on emulsion structure and size distribution, which is desired for various biological and pharmaceutical applications.

Acknowledgments

This work was supported in part by the National Science Council of Taiwan under Contract No. NSC 95-2221-E-007-226. The demonstrated systems were fabricated in the ESS Microfabrication Lab at National Tsing Hua University, Taiwan.

References

[1] Becher P 1965 *Emulsions: Theory and Practice* (New York: Van Nostrand-Reinhold)

[2] Lissant K J 1974 *Emulsion and Emulsion Technology* (New York: Dekker)

[3] Schramm L L 2005 *Emulsions, Foams, and Suspensions: Fundamentals and Applications* (Weinheim: Wiley)

[4] Benita S 1996 *Microencapsulation: Methods and Industrial Application* (New York: Dekker)

[5] Thorsen T, Roberts R W, Arnold F H and Quake S R 2001 Dynamic pattern formation in a vesicle-generating microfluidic device *Phys. Rev. Lett.* **86** 4163–6

[6] Nisisako T, Torii T and Higuchi T 2002 Droplet formation in a microchannel network *Lab Chip* **2** 24–6

[7] Dendukuri D, Tsoi K, Hatton T A and Doyle P S 2005 Controlled synthesis of nonspherical microparticles using microfluidics *Langmuir* **21** 2113–6

[8] Ganan-Calvo A M 1998 Generation of steady liquid microthreads and micron-sized monodisperse sprays in gas streams *Phys. Rev. Lett.* **80** 285–8

[9] Umbanhowar P B, Prasad V and Weitz D A 2000 Monodisperse emulsion generation via drop break off in a coflowing stream *Langmuir* **16** 347–51

[10] Ganan-Calvo A M and Gordillo J M 2001 Perfectly monodisperse microbubbling by capillary flow focusing *Phys. Rev. Lett.* **87** 274501

[11] Anna S L, Bontoux N and Stone H A 2003 Formation of dispersions using ‘flow focusing’ in microchannels *Appl. Phys. Lett.* **82** 364–6

[12] Garstecki P, Gitlin I, DiLuzio W and Whiteside G M 2004 Formation of monodisperse bubbles in a microfluidic flow-focusing device *Appl. Phys. Lett.* **85** 2649–51

[13] Tan Y C, Fisher J S, Lee A I, Cristini V and Lee A P 2004 Design of microfluidic channel geometries for the control of droplet volume, chemical concentration, and sorting *Lab Chip* **4** 292–8

[14] Dreyfus R, Tabeling P and Willaime H 2003 Ordered and disordered patterns in two-phase flows in microchannels *Phys. Rev. Lett.* **90** 144505

[15] Barbier V, Tatoulian M, Li H, Arefi-Khonsari F, Ajdari A and Tabeling P 2006 Stable modification of PDMS surface properties by plasma polymerization: application to the formation of double emulsions in microfluidic systems *Langmuir* **22** 5230–2

[16] Seo M, Paquet C, Nie Z, Xu S and Kumacheva E 2007 Microfluidic consecutive flow-focusing droplet generators *Soft Matter* **3** 986–92

[17] Goubault C, Pays K, Olea D, Gorria P, Bibette J, Schmitt V and Leal-Calderon F 2001 Shear rupturing of complex fluids: application to the preparation of quasi-monodisperse water-in-oil-in-water double emulsions *Langmuir* **17** 5184–8

[18] Mishra B and Pandit J K 1989 Prolonged release of pentazocine from multiple o/w/o emulsions *Drug Dev. Ind. Pharm.* **15** 1217–30

[19] Ferreira L A M, Seiller M, Grossiord J L, Marty J P and Wepierre J 1994 Vehicle influence on in vitro release of metronidazole: role of w/o/w multiple emulsion *Int. J. Pharm.* **109** 251–9

[20] Lim F and Sun A M 1980 Microencapsulated islets as bioartificial endocrine pancreas *Science* **210** 908–10

[21] Fritschy W M, Wolters G H and van Schilfgaarde R 1991 Effect of alginate-polylysine-alginate microencapsulation on *in vitro* insulin release from rat pancreatic islets *Diabetes* **40** 37–43

[22] Dusseault J, Leblond F A, Robitaille R, Jourdan G, Tessier J, Menard M, Henley N and Halle J P 2005 Microencapsulation of living cells in semi-permeable membranes with covalently cross-linked layers *Biomaterials* **26** 1515–22

[23] Okushima S, Nisisako T, Torii T and Higuchi T 2004 Controlled production of monodisperse double emulsions by two-step droplet breakup in microfluidic devices *Langmuir* **20** 9905–8

[24] Berkland C, Pollauf E, Pack D W and Kim K 2004 Uniform double-walled polymer microspheres of controllable shell thickness *J. Control Release* **96** 101–11

[25] Bocanegra R, Sampedro J L, Ganan-Calvo A and Marquez M 2005 Monodisperse structured multi-vesicle microencapsulation using flow-focusing and controlled disturbance *J. Microencapsul.* **22** 745–59

[26] Utada A S, Lorenceau E, Link D R, Kaplan P D, Stone H A and Weitz D A 2005 Monodisperse double emulsions generated from a microcapillary device *Science* **308** 537–41

[27] Huang S H, Tan W H, Tseng F G and Takeuchi S 2006 A monolithically three-dimensional flow-focusing device for formation of single/double emulsions in closed/open microfluidic systems *J. Micromech. Microeng.* **16** 2336–44

[28] Takeuchi S, Garstecki P, Weibel D B and Whitesides G M 2005 An axisymmetric flow-focusing microfluidic device *Adv. Mater.* **17** 1067–72

[29] Yobas L, Martens S, Ong W L and Ranganathan N 2006 High-performance flow-focusing geometry for spontaneous generation of monodispersed droplets *Lab Chip* **6** 1073–9

[30] Clanet C and Lasheras J C 1999 Transition from dripping to jetting *J. Fluid Mech.* **383** 307–26

[31] Ambravaneswaran B, Subramani H J, Phillips S D and Basaran O A 2004 Dripping-jetting transitions in a dripping faucet *Phys. Rev. Lett.* **93** 034501

[32] Utada A S, Chu L Y, Fernandez-Nieves A, Link D R, Holtze C and Weitz D A 2007 Dripping, jetting, drops, and wetting: the magic of microfluidics *MRS Bull.* **32** 702–8

[33] Duffy D C, McDonald J C, Schueller O J A and Whitesides G M 1998 Rapid prototyping of microfluidic systems in poly(dimethylsiloxane) *Anal. Chem.* **70** 4974–84

[34] Anderson J R, Chiu D T, Jackman R J, Cherniavskaya O, McDonald J C, Wu H, Whitesides S H and Whitesides G M 2000 Fabrication of topologically complex three-dimensional microfluidic systems in PDMS by rapid prototyping *Anal. Chem.* **72** 3158–64

[35] Sundararajan N, Pio M S, Lee L P and Berlin A A 2004 Three-dimensional hydrodynamic focusing in polydimethylsiloxane micro-channels for molecular detection *J. Microelectromech. Syst.* **13** 559–67

[36] Haubert K, Drier T and Beebe D 2006 PDMS bonding by means of a portable, low-cost corona system *Lab Chip* **6** 1548–9

[37] Adamson A W and Gast A P 1997 *Physical Chemistry of Surfaces* (New York: Wiley)